Evaluation of the Forward Scattering Spectrometer Probe. Part II: Corrections for Coincidence and Dead-Time Losses

DARREL BAUMGARDNER

Research Aviation Facility, National Center for Atmospheric Research, Boulder, CO*

WALTER STRAPP

Atmospheric Environment Service, Toronto, Ontario, Canada

JAMES E. DYE

Convective Storms Division, National Center for Atmospheric Research, Boulder, CO*

(Manuscript received 4 October 1984, in final form 7 June 1985)

ABSTRACT

Cloud particle concentrations measured by the Forward Scattering Spectrometer Probe (FSSP) can be underestimated when particles are either coincident or pass through the sensing area of the probe during the electronic dead-time. In the absence of any corrections, the differences between actual and measured concentrations can typically exceed 15% when aircraft mounted probes measure droplet concentrations > 500 cm^{-3}. The sources of counting losses are described and correctional procedures derived and demonstrated.

1. Introduction

As originally discussed by Cooper (1978) and more recently by Dye and Baumgardner (1984), particle concentrations measured by the Forward Scattering Spectrometer Probe (FSSP) are underestimated when particles pass through the sample area undetected. These losses arise when particles are coresident in the beam (coincidence event) or when particles pass through the laser beam during an electronic delay period following each detected particle when the electronics of the probe are blind to subsequent particle arrivals (dead-time event). Although this problem has been recognized for several years, there has been confusion regarding the magnitude of these losses and the method by which compensation may be made. In this paper we discuss the nature of these losses and, by statistically estimating their frequency, derive corrections which can be applied to decrease the measurement errors.

Descriptions of the operation of the FSSP are presented by Knollenberg (1981) and Dye and Baumgardner (1984). To understand the following work we briefly review aspects germane to this presentation. The FSSP counts and sizes individual particles by measuring the intensity of light that is forward-scattered as each particle passes through a laser beam. The scattered light passes through a prism and collecting lens and enters a beam-splitting prism. One portion of the light from the prism illuminates a photodetector, which is referred to as the signal detector, while the other portion falls on a detector that has been partially masked to respond to only that light from the larger scattering angles and is referred to as the annulus. Particles passing through the beam far from the focal plane scatter proportionally more light into the annulus than those close to the focal plane. Thus, the depth-of-field (DOF) can be established by an electronic comparison of the annulus and signal voltages.

To reject particles that pass through the edges of the beam where the laser intensity is diminished and undersizing may occur, an electronic average is maintained of the transit times of all particles passing within the DOF. Particles whose transit times are shorter than this average are rejected since they are probably those that passed near the laser edges. The effective beam diameter used for calculating sample area is thus only a fraction of the actual diameter.

After a particle passes completely through the beam, a fixed delay period is initiated during which size information is transferred to the data system and the electronics are reset in preparation for the next event.

2. Coincidence losses

When more than a single particle is present in the beam at any time, the electronics of the FSSP can dis-

* The National Center for Atmospheric Research is sponsored by the National Science Foundation.

criminate only one. The effect of this coincidence event depends upon where the particles are positioned relative to the DOF and their respective sizes. Referring to Fig. 1, the probe's laser beam consists of three different areas: the DOF, the region where the annulus output is greater than the peak signal (area 1), and the outer region (area 2). The distinction between these three areas is important to an understanding of the types of coincidence events and the resultant effect on measurements. Four types of coincidence events can occur depending upon the relative position of coresident particles in the three areas of the beam.

1) Since only those particles that pass through the DOF are used for calculating measured concentrations, particles coincident but outside the DOF will cause no counting errors. (They will, however, still contribute to the cumulative dead-time during the sampling period.)

2) If more than one particle is coresident in the DOF, the particles will be counted as one.

3) If one particle is within the DOF and another in area 1, the particle in the DOF will not be counted if, after normalizing for the gain, the annulus output caused by the combined scattered light from the out-of-DOF and in-DOF particles is larger than the signal output caused by the same particles' combined light. From Fig. 1 it can be seen that the effect of this type of coincidence event depends on the relative size of the particles and where they pass through the DOF and area 1.

4) This event is the same as event 3, except the particle outside the DOF is in area 2 and does not cause the FSSP to ignore the particle in the DOF; therefore no counting losses will occur.

Coincidence events can also affect the sizing of particles as a result of the combined scattered light from the coresident particles in the beam. Although the resulting size is probably an overestimate, the complex nature of the scattering makes it difficult to determine the error. The effective beam diameter measured by the velocity averaging circuit can also be biased by coincidence events; however such errors are probably secondary to other uncertainties that exist in the determination of sample volume (Dye and Baumgardner, 1984).

3. Electronic dead-time losses

As illustrated in Fig. 2, a particle will not be counted if it passes through the sample area during the electronic delay sequence which follows the detection of the previous particle (particle D in Fig. 2). However, if the particle enters the sample area during the delay sequence, but remains in the beam when the electronics are reset, the FSSP will detect it (particle G in Fig. 2).

4. Estimation of particle losses

An estimate can be made of the actual concentration from the measured concentration if certain optical and electronic characteristics of the probe are known. This derivation takes the general form

$$n_a = n_m + n_c + n_d, \tag{4.1}$$

where n_a and n_m are the actual and measured number

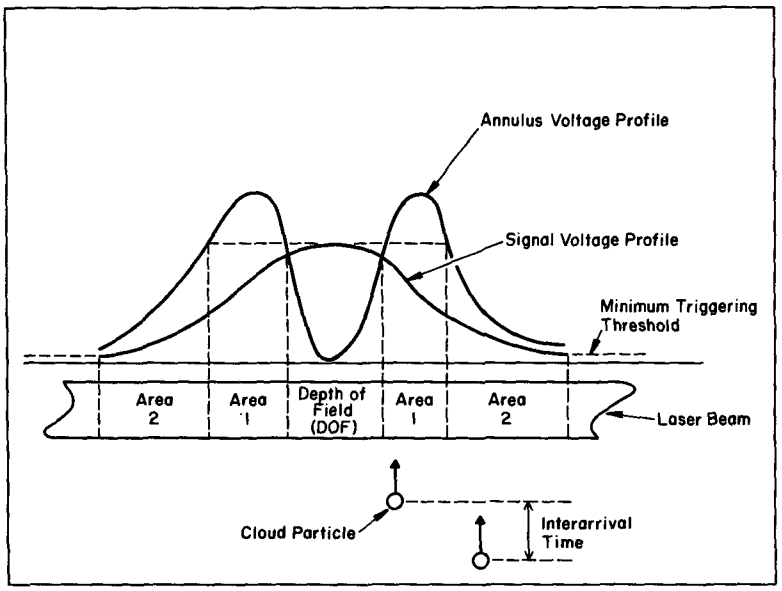

FIG. 1. This graphical representation of the FSSP laser beam depicts the relative magnitudes of the annulus and scattering voltages that result from particles passing through different parts of the beam.

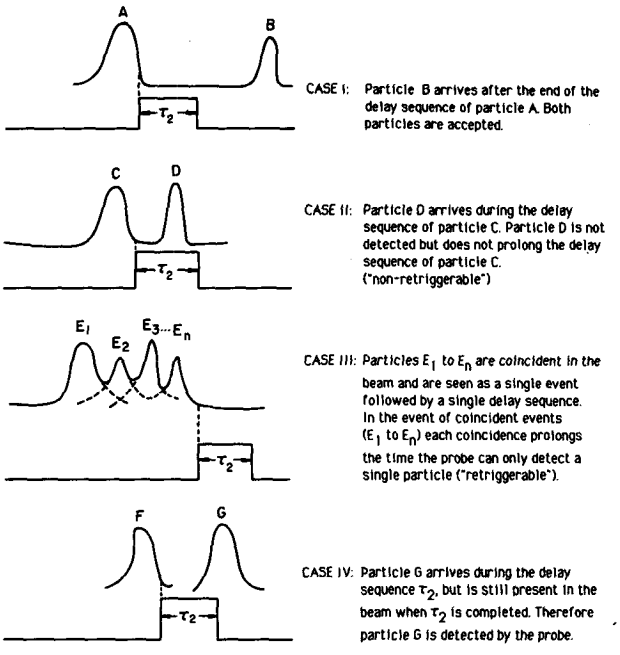

FIG. 2. Schematic representation of coincidence and dead-time events with respect to the timing in the FSSP.

of particles per unit sample time passing through the DOF and n_c and n_d are the particles undetected because of coincidence and dead-time during the same sampling period.

The FSSP is an instrument that counts individual particles. Much has been written concerning the operating characteristics of such devices: in particular, the problems concerning losses resulting from coincidence and electronic dead-time. For example, Feller (1950) provides a solid theoretical explanation of renewal processes while Westcott (1948) gives a more applications-oriented treatise. In general, the dead-time mechanism of a counter may take one of two forms. The inoperative period may follow only those counts (particles) that are recorded (Type I or nonretriggerable counter), or it may follow all counts, including those suppressed by the dead period after a previous count, thus lengthening the total dead period until a time after the last count to be recorded (Type II or retriggerable counter).

The FSSP behaves as both a Type I and II counter. The period of time that a particle is resident in the beam can be considered a dead period for more than a single arrival since other particles entering during this period will be indistinguishable from the first particle (Fig. 2, case II). Since particles coincident in the beam may lengthen this dead period, this part of the FSSP's operation can be treated like a Type II counter. Once the particle(s) have cleared the beam, a fixed delay period is initiated which cannot be prolonged by additional particles passing through the beam; hence, the FSSP functions as a Type I counter during this phase of operation (Fig. 2, case II). In early models of the FSSP and ASSP this delay sequence was retriggerable, but, to the best of our knowledge, modifications have been made to all probes so that, currently, the delay sequence is not retriggerable.

Using the statistical methods developed for estimating the Type I and II losses, we can now estimate the quantities n_d and n_c in (4.1).

a. Estimation of coincidence losses

The probability of a coincidence event can be determined if we assume the particles are located randomly in space and that the probability density function for particles arriving at time t after a previous particle has entered the beam is given by the exponential probability density function

$$f(t) = \lambda e^{-\lambda t} \tag{4.2}$$

where λ is the expected (mean) interarrival rate of particles (Meyer, 1965). A particle will be coresident with another particle if it arrives within a period less than or equal to the transit time of the previous particle (as illustrated by the timing diagram shown in Fig. 2). The probability of this occurrence is found by integrating and evaluating (4.2) between zero and τ_1, the average transit time of a particle:

$$P_t = P(0 < t \leq \tau_1) = \int_0^{\tau_1} \lambda e^{-\lambda t} dt, \tag{4.3}$$

$$= 1 - e^{-\lambda \tau_1}. \tag{4.4}$$

The mean arrival rate is

$$\lambda = \lambda_1 + 2\lambda_2. \tag{4.5}$$

As described in the second section, coincidence losses result from two types of particle interactions. These effects are reflected in the calculated mean arrival rates λ_1 and λ_2. For the case of particles coincident in the DOF, the mean arrival rate is

$$\lambda_1 = N_a W v L_D, \tag{4.6}$$

where N_a is the actual concentration, W is the beam width, L_D is the length of the DOF, and v is the true airspeed.

The second type of coincidence event can occur either when a particle is in the DOF followed by a particle outside the DOF, or alternately a particle can enter the DOF while the previous particle is outside the DOF. Hence the need for the factor of 2 in (4.6). For this case

$$\lambda_2 = N_a W v L_1, \tag{4.7}$$

where L_1 is the length of the beam in area 1. Combining (4.6) and (4.7) results in

$$\lambda = N_a W v (L_D + 2L_1). \tag{4.8}$$

The best estimate of the average transit period τ_1 is the average beam chord divided by the true airspeed, where

the average beam chord found by simple calculus is 78% of the beam diameter.

The mean arrival rate λ is an approximation since, as previously discussed, it does not take into account the respective size and position of coresident particles in the DOF and area 1. Although (4.5) could be further refined to account for these effects, such an effort seems unjustifiable in light of other uncertainties that limit the measurement accuracy of this probe (Baumgardner, 1983; Dye and Baumgardner, 1984).

Equation (4.4) is the probability of any coincidence event that can influence particle counting. However, because coincidence events during the delay sequence τ_2 are treated separately as dead-time losses in the following section, we must determine the probability that a coincident event has occurred and that it did not occur during the electronic delay sequence. Assuming these are independent events, the resulting probability is

$$P_c = P_t(1 - P_d) \tag{4.9}$$

where P_d is the probability of a dead-time event occurring during the sample period.

For large n_c and n_a, n_c may be approximated using the relative frequency, f_c, which is the fraction of total particles that are coincident:

$$n_c = n_a f_c \approx n_a P_c = n_a(1 - e^{-\lambda\tau_1})(1 - P_d). \tag{4.10}$$

b. Estimation of dead-time losses

The dead-time losses can be estimated using an actual measurement of the cumulative dead-time of the probe over a given sampling period. Feller (1950) shows that the expected number of counts, n_e, measured by a purely nontriggerable counter will be

$$n_e = n_a\left(\frac{T - \tau}{T}\right) \tag{4.11}$$

where τ is the accumulated dead-time during the sample period, T. Since n_d is the difference between the actual and expected number of counts, (4.11) can be rearranged to get

$$n_d = \frac{n_a\tau}{T}. \tag{4.12}$$

The relative frequency f_d of dead-time losses is the ratio of n_d to n_a and for large n_d and n_a is a good approximation to the probability P_d (Meyer, 1965).

$$P_d \approx f_d = \frac{n_d}{n_a} = \frac{\tau}{T}. \tag{4.13}$$

The cumulative dead-time τ can be estimated if there are separate measurements of n_m, all particles passing inside the DOF (also known as "total strobes") and n_0, all other particles detected during the sampling period (also called "fast resets"). The cumulative dead-time during which particles can be lost is then

$$\tau = n_m(\tau_2 - \tau_1) + n_0(\tau_3 - \tau_1), \quad \tau_3 > \tau_1, \tag{4.14}$$

$$\tau = n_m(\tau_2 - \tau_1), \quad \tau_3 < \tau_1, \tag{4.15}$$

where τ_2 and τ_3 are the slow and fast delay times, respectively. (Some probes only use a slow delay in which case $\tau_3 = \tau_2$.) The average transit time, τ_1, must be subtracted from each delay since a particle is only missed if it arrives before the end of the delay a length of time greater than the amount of time it would take to transit the beam (see Fig. 2, Case IV). The dead-time estimated in (4.14) and (4.15) will be slightly less than the actual dead-time since n_m only includes those particles that were in the sizing range of the FSSP. Particles smaller or larger than the FSSP size thresholds will also cause electronic delays; however, not counting these particles when estimating the dead-time is expected to cause less than 10% errors.

If n_0 and n_m are not measured, they can be estimated from the measured concentration, N_m:

$$n_m = WL_D v N_m T, \tag{4.16}$$

$$n_0 = \frac{(L_0 - L_D)n_m}{L_D}, \tag{4.17}$$

where L_0 is the total sensitive beam length which is a function of particle size and individual probe optics and is typically 15–20 mm.

c. Correction algorithms

Substituting (4.10) and (4.12) in (4.1), dividing through by sample volume, and rearranging gives the following equation describing the relation of measured and actual concentration for combined coincidence and deadtime losses.

$$N_m = N_a\frac{(T - \tau)e^{-\lambda\tau_1}}{T}. \tag{4.18}$$

Note that this equation reduces to the expected expressions for a simple retriggerable or nonretriggerable counter by setting τ_1 and τ to zero, respectively.

To solve directly for N_a requires an iterative procedure since N_a is also in the exponential term. However, for $\lambda\tau_1 \ll 1$, the exponential may be approximated as

$$e^{-\lambda\tau_1} = 1 - \lambda\tau_1, \tag{4.19}$$

and (4.18) can be written as

$$\tau_1 W\left(1 - \frac{\tau}{T}\right)(L_D + L_1)vN_a^2 - \left(1 - \frac{\tau}{T}\right)N_a + N_m = 0, \tag{4.20}$$

which has real roots as long as

$$\left(1 - \frac{\tau}{T}\right) > 4\tau_1 WvN_m(L_D + L_1). \tag{4.21}$$

The magnitudes of coincidence and dead-time losses n_c and n_d are shown graphically in Fig. 3, where they are plotted as a percentage of the total number of particles passing through the viewing volume. In this example, W =0.2 mm, L_D = 3.0 mm, L_0 = 15.0 mm, L_1 = 3.0 mm, v = 100 m s^{-1}, τ_2 = 6.0 μs, τ_3 = 2.8 μs and T = 1 s. For this case the percentage of particles lost during the dead-time period is typically about 10% greater than the coincidence losses. However, the relationship between coincidence and dead-time losses is a sensitive function of airspeed and delay times, such that sometimes the coincidence losses can be larger than the dead-time losses.

The behavior of correction equations (4.18) and (4.20) can be seen in Fig. 4. Comparing the iterative to the quadratic solution it can be seen that both solutions are within good agreement until the actual and measured concentrations exceed about 350 and 250 cm^{-3}, respectively. The concentration at which the solutions begin to diverge is a function of a particular FSSP's optical and electronic configuration as well as the airspeed.

For the probe configuration used in Fig. 4 the point at which the measured concentration from the iterative solution reaches a maximum is about 1300 cm^{-3}, while the maximum is around 600 cm^{-3} for the quadratic correction equation. Neither (4.18) or (4.20) are monotonic functions; hence, measured concentrations can be produced by two different actual concentrations. From physical considerations, however, it would be extremely rare to have natural particle concentrations

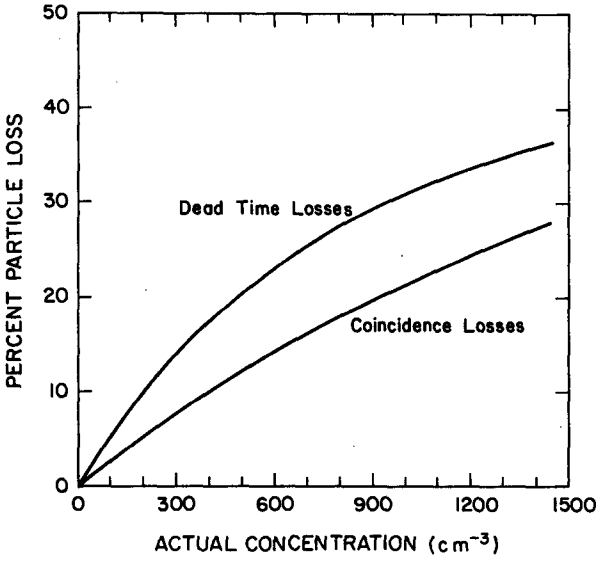

FIG. 3. The number of particles undetected by the FSSP are shown as percentages of the total number of particles that passed through the same volume during a given sampling period. The curves represent an evaluation of (4.10) and (4.12),where W = 0.2 mm, L_D = 3.0 mm, L_0 = 15.0 mm, L_1 = 3.0 mm, v = 100 m s^{-1}, τ_2 = 6.0 μs, τ_3 = 2.8 μs.

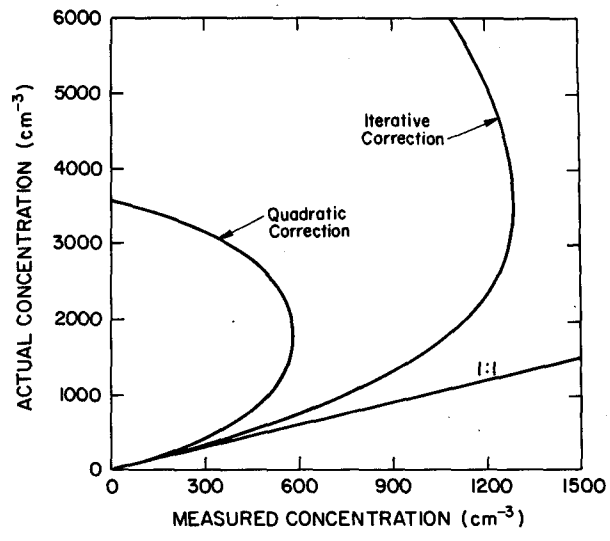

FIG. 4. Using the same values for W, L_D, L_0, L_1, τ_1, τ_2, and τ_3 as in Fig. 3, the iteratively and quadratically corrected concentrations are plotted as a function of measured concentration.

sufficiently large to produce such ambiguities. In general, as seen in Fig. 4, the iterative solution should be used for the most accurate corrections.

As a practical application, the correction equations were applied to FSSP measurements of a water droplet spray in a wind tunnel. The relative droplet concentrations in the tunnel were controlled by varying the water flow rate; however,there was no way of determining by other methods what the actual droplet concentrations were. The estimated actual concentrations derived using both correction methods are shown as a function of the measured concentration in Fig. 5. Differences in the two correction techniques are scarcely detectable until the measured concentrations exceed about 300 cm^{-3}. Also plotted on this figure are the estimates of the actual concentration using n_m and n_0 derived from the measured concentration as detailed in (4.16) and (4.17).

Previous corrections for coincidence and dead-time losses have been made using the measured activity, an output provided by PMS on later versions and some modified earlier versions of the probe. As incorporated by PMS, the activity A is the fraction of the sampling period that the FSSP is actively processing particles and includes the sum of the transit and delay times for each particle that transits the beam during the sample period. The activity is somewhat analogous to equation (4.13), the ratio of the cumulative dead-times to sample period, with the distinction that in (4.13) the particle transit time is subtracted from each delay sequence and, hence, is not included in the accumulated dead-time τ. The correction equation, which was first proposed by PMS and modified by Baumgardner (1983), takes the form

$$N_m = N_a(1 - mA), \qquad (4.22)$$

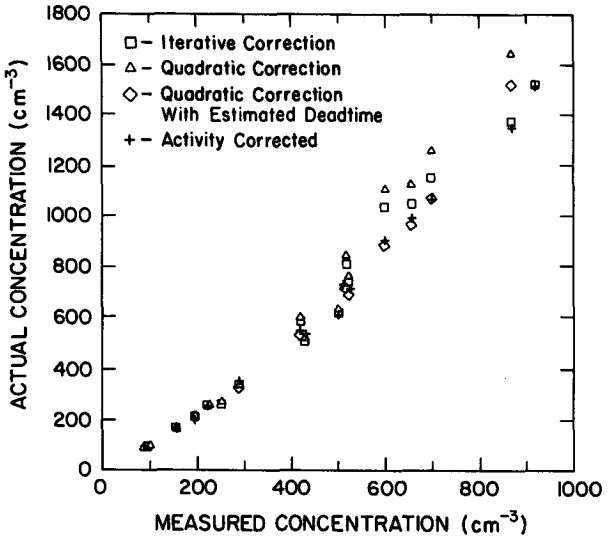

FIG. 5. The correction equations are applied to measurements taken with an FSSP in a wind tunnel at three air speeds, v = 60, 80, 100 m s^{-1} and a wide range of liquid water values. The probe's optical and electronic configuration is w = 0.20 mm, L_D = 3.00 mm, L_0 = 15 mm, L_1 = 3.0 mm, τ_2 = 6.0 μs, and τ_3 = 2.8 μs.

where m is a probe-dependent correction factor to the activity determined experimentally by PMS. Equation (4.22) has a form similar to (4.18); however, in (4.22) the coincidence and dead-time corrections are combined into a single empirical correction and are not treated explicitly. The factor m was added after it was realized that the corrected concentrations were being overestimated. The manufacturer suggests a correction factor of 0.7 to 0.8; however, simulations of the physical operation of the FSSP show that the value of m for each probe depends upon the optical and electronic characteristics of individual FSSPs as described by Dye and Baumgardner (1984). The values of the corrected concentration using (4.22) and a value for m of 0.54 derived from laboratory simulations (Cerni, 1983) for this probe are plotted in Fig. 5 along with the iterative and quadratic corrections described earlier. If (4.18) is used to estimate N_a, another value for m can be derived by rearranging (4.22) in the form of a linear equation

$$\frac{N_a - N_m}{N_a} = mA. \tag{4.23}$$

The slope of the best-fit line is then an approximation to the value of m, which in this case, as shown in Fig. 6, is 0.65. This value is in good agreement with the laboratory or computer-simulated values. The scatter seen in Fig. 6 gives a feeling of the accuracy with which corrections can be made to measured concentrations by the use of the activity correction.

5. Summary, conclusions and recommendations

A large source of uncertainty with particle concentration measurements from the FSSP is the inability of the probe to detect particles coresident in the beam or particles that pass through the beam during the electronic dead-time. A statistical correction procedure was developed from an analysis of the FSSP's operating characteristics with the use of a few approximations and assumptions. Specifically, the cloud particles were assumed to be randomly distributed in space and to pass through the laser beam with the same average transit time for a given airspeed and beam width. Additionally, it was shown that the sensitive beam length can be described by three areas, within which four types of coincidence interactions occur.

The most exact correction technique requires an iterative solution; however, an approximate analytical solution was demonstrated for a typical FSSP that was within 10% of the iterative value when measured concentrations were less than approximately 400 cm^{-3}. Although recording total strobes and fast resets (or total resets) as additional output information was recommended, the correction techniques can be applied with the basic information provided by unmodified FSSPs.

In conclusion, the techniques developed to correct FSSP measurements for undetected particles may not be exact because of the assumptions necessary for deriving the statistical equations. However, since FSSP measurements of moderately high concentrations can be substantially in error because of coincidence and dead-time losses, these correction procedures should significantly decrease the uncertainties in these measurements. Experimental verification is still needed before we can assess the error introduced by the assumptions used in deriving these corrections.

It is the recommendation of the authors that users of the FSSP select a correction technique based upon

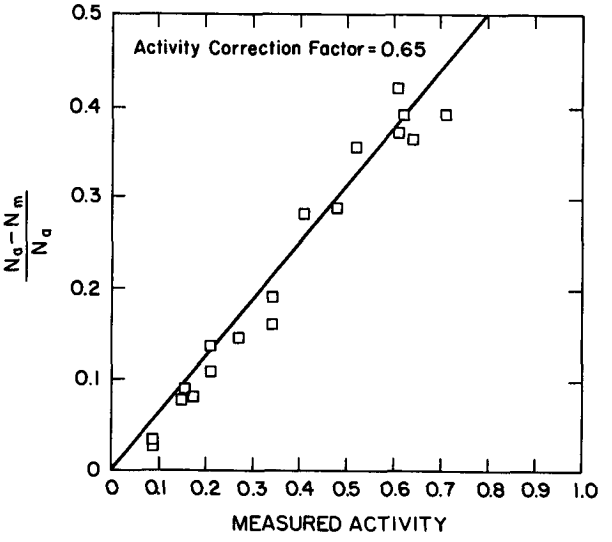

FIG. 6. Percent difference between statistically corrected concentration and measured concentration as a function of the measured activity for the probe whose measurements are shown in Figs. 3–5. The slope of the best-fit line is the estimated value of the factor m.

the information available from their probe. In particular, if the total strobes and fast resets are an option with their FSSP, they should apply the iterative or quadratic statistical corrections to their data. If activity is recorded, the correction equation should take the form of (4.22), with an m value determined as in Fig. 6. For those users with no auxiliary parameters, the total strobes and fast resets can be determined as outlined in (4.16) and (4.17). Finally, all the correction techniques require an accurate measure of the electronic delay time and dimensions of the laser beam's diameter and depth-of-field for any particular FSSP.

Acknowledgments. The authors would like to express thanks to Warren King, Cleon Biter, and W. A. Cooper for their meticulous reviews of the manuscript and subsequent enlightening discussions.

APPENDIX

Nomenclature and List of Symbols

DOF optical depth-of-field of the FSSP (mm),
L_D length of the depth-of-field,
L_0 the total sensitive laser beam length of the FSSP (mm),
L_1 the length of laser beam in area one (mm),
n_a actual number of particles passing through the DOF during a given time period,
n_c the number of particles undetected during a given time period because of coincidence in the beam but not occurring during an electronic delay period,
n_d the number of particles undetected during a given time period because of the electronic dead-time,
n_e the expected number of particles in absence of coincidence losses,
n_m all particles detected within the DOF during a given time period,
n_0 all particles detected outside the DOF during a given time period,
N_a actual particle concentration (cm^{-3}),
N_m measured particle concentration (cm^{-3}),
P_c probability of coincidence events,
P_d probability of dead-time events,
t the time between the arrival of particles in the FSSP viewing volume (s),
T sampling period during which counts are measured (s),
v the speed of particles passing through the FSSP viewing volume ($m\ s^{-1}$),
W width of the laser beam (mm),
λ average arrival rate of particles in the laser beam (s^{-1}),
τ cumulative electronic dead-time during sampling period (μs),
τ_1 average transit time of particles through laser beam (μs),
τ_2 electronic delay time of electronics for particles passing through DOF (μs), and
τ_3 electronic delay time of electronics for particles passing outside the DOF (μs).

REFERENCES

Baumgardner, D., 1983: An analysis and comparison of five water droplet measuring instruments. *J. Appl. Met.*, **22,** 891–910.

Cerni, T. A., 1983: Determination of the size and concentration of cloud drops with an FSSP. *J. Appl. Met.*, **22,** 1346–1355.

Cooper, W. A., 1978: Cloud physics investigations at the University of Wyoming in HIPLEX 1977. U. Wyo. Atmos. Sci. Rpt. AS119, 320 pp.

Dye, J. E., and D. Baumgardner, 1984: Evaluation of the forward scattering spectrometer probe. Part I: Electronic and optical studies. *J. Atmos. Oceanic Technol.*, **1,** 329–344.

Feller, W., 1950: *An introduction to probability theory and its applications, Volume I.* John Wiley & Sons, 461 pp.

Knollenberg, R. G., 1981: Techniques for probing cloud microstructure. *Clouds, Their Formation, Optical Properties, and Effects,* P. V. Hobbs and A. Deepak, Eds., Academic Press, 495 pp.

Meyer, P. L., 1965: *Introductory probability and statistical applications.* Addison Wesley Publishing Co., 339 pp.

Westcott, C. H., 1948: A study of expected loss rates in the counting of particles from pulsed sources. *Proc. Roy. Soc. London, Series A,* **194,** 508–526.